



HAL
open science

PdZn or ZnPd: Charge transfer and Pd-Pd bonding as the driving force for the tetragonal distortion of the cubic crystal structure

Matthias Friedrich, Alim Ormeci, Juri Grin, Marc Armbrüster

► **To cite this version:**

Matthias Friedrich, Alim Ormeci, Juri Grin, Marc Armbrüster. PdZn or ZnPd: Charge transfer and Pd-Pd bonding as the driving force for the tetragonal distortion of the cubic crystal structure. *Journal of Inorganic and General Chemistry / Zeitschrift für anorganische und allgemeine Chemie*, 2010, 636 (9-10), pp.1735. 10.1002/zaac.201000097 . hal-00552466

HAL Id: hal-00552466

<https://hal.science/hal-00552466>

Submitted on 6 Jan 2011

HAL is a multi-disciplinary open access archive for the deposit and dissemination of scientific research documents, whether they are published or not. The documents may come from teaching and research institutions in France or abroad, or from public or private research centers.

L'archive ouverte pluridisciplinaire **HAL**, est destinée au dépôt et à la diffusion de documents scientifiques de niveau recherche, publiés ou non, émanant des établissements d'enseignement et de recherche français ou étrangers, des laboratoires publics ou privés.



PdZn or ZnPd: Charge transfer and Pd-Pd bonding as the driving force for the tetragonal distortion of the cubic crystal structure

Journal:	<i>Zeitschrift für Anorganische und Allgemeine Chemie</i>
Manuscript ID:	zaac.201000097.R1
Wiley - Manuscript type:	Article
Date Submitted by the Author:	06-Apr-2010
Complete List of Authors:	Friedrich, Matthias; Max-Planck-Institut für Chemische Physik fester Stoffe Ormeci, Alim; Max-Planck-Institut für Chemische Physik fester Stoffe Grin, Juri; Max-Planck-Institut für Chemische Physik fester Stoffe Armbrüster, Marc; Max-Planck-Institut für Chemische Physik fester Stoffe
Keywords:	ZnPd, PdZn, Chemical bonding, ELI, Homogeneity range



1
2
3 **PdZn or ZnPd: Charge transfer and Pd-Pd bonding as the driving force for the**
4 **tetragonal distortion of the cubic crystal structure**
5
6
7

8 Matthias Friedrich, Alim Ormeci, Yuri Grin, Marc Armbrüster[#]
9

10
11
12 [#]corresponding author, e-mail: research@armbruester.net, Max-Planck-Institut für
13 Chemische Physik fester Stoffe, Nöthnitzer Str. 40,
14 01187 Dresden, Germany
15
16
17
18

19
20 Dedicated to the 60th birthday of Prof. Dr. Bernd Harbrecht
21
22

23 **Abstract:**
24

25 The intermetallic compound PdZn was reported to possess two modifications, the
26 tetragonal CuAu-type low-temperature phase and the cubic CsCl-type high-
27 temperature phase. The existence of the cubic high-temperature phase at the
28 equiatomic composition could not be proven experimentally. Calculations of the total
29 energy reveal a minimum at $c/a = 1.155$, clearly excluding the cubic structure at the
30 equiatomic composition in the system Pd-Zn. Analysis of the chemical bonding
31 applying the electron localizability approach reveals charge transfer from Zn to Pd
32 and proves direct Pd-Pd interactions in the (001) plane to be the main reason for the
33 tetragonal distortion of the cubic CsCl-type structural pattern for ZnPd.
34
35
36
37
38
39
40
41
42

43 **Keywords:** PdZn, ZnPd, chemical bonding, ELI, homogeneity range
44
45
46
47
48
49
50
51
52
53
54
55
56
57
58
59
60

Introduction

The tetragonal distortion of the CsCl type of structure towards the CuAu type of structure has been subject of debate over several decades. *Johansson* and *Linde* were the first to explain the tetragonal lattice of CuAu by ascribing the distortion to the different atomic radii of Cu and Au [1]. *Schubert* showed that the ratio of the atomic radii does not linearly correlate with the ratio of the axes [2]. Hence, the influence of the atomic radii seemed not to be the only driving force for the distortion. The argument, that the tetragonal lattice is formed due to favoured heteroatomic interactions like in tetragonal NiZn [3] – one Ni atom is surrounded by eight Zn atoms, but only by four Ni atoms – was rejected by comparison to PtCu. The latter is not distorted tetragonally, it is slightly rhombohedral; every atom is surrounded by 6 atoms of each kind [2]. *Dehlinger* suggested another driving force for the distortion [4]. The tetragonal lattice results in new Brillouin zones leading to additional Bragg reflections. Since these allow accommodating electrons in an energetically favourable way, the Fermi energy is decreased by the distortion. Counter arguments for this thesis are supported by the crystal structures of NiZn, PdCd and PtHg which do not show intense additional reflections but still form the CuAu type of structure. *Schubert's* model of the *Ortskorrelation* [2] tried to explain the tetragonal structure by the contribution of a certain number of valence electrons of each atom to stabilization of the crystal structure. *Neumann et al.* analysed several compounds realizing the CuAu structure for influence of ionic bonding on the structure. Results showed a correlation between the degree of tetragonality and the enthalpy of formation or degree of ionic bonding, respectively [5]. However, this is contradictory since ionic interactions should favour the more isotropic undistorted CsCl-type. Experimental and quantum chemical investigations of TiAl (CuAu type of structure) resulted in the description of covalently bonded Ti 4^d nets in the structure to which the tetragonal distortion was assigned [6, 7]. High-pressure experiments on CuAu [8] revealed that the atomic size ratio plays only a secondary role for the tetragonality in CuAu type structures. More important are band structure effects, resulting in an energetically favourable way to accommodate the electrons. As already suggested by *Schubert* [2] and *Neumann et al.* [5], a single aspect might not solely explain the tetragonal distortion in CuAu type structures.

1
2
3 The equiatomic phase in the binary system Pd-Zn is usually described with the
4 formula PdZn. The tetragonal structure of the room temperature modification was first
5 reported in 1950 by *Nowotny et al.* [9]. Later *Nowotny et al.* [10] and *Köster et al.*
6 [11] investigated the high temperature region at the composition Pd₂Zn and Pd₂Zn₃
7 both of which realize the cubic CsCl structure type. The authors remained unsure,
8 whether the phase ranges of Pd₂Zn and Pd₂Zn₃ merge at high temperatures or if two
9 separate phases exist. To our best knowledge, no experimental evidence of the cubic
10 CsCl-type crystal structure at 50 at.-% Pd at elevated temperatures has been reported
11 so far. The latest cumulative phase diagram in [12] is based on earlier work of [13]
12 where the high temperature region is shown as tentative.

13
14 Investigating chemical bonding by means of electron localization approach has
15 proven to be an efficient tool in exploring chemical stability and catalytic properties
16 of intermetallic compounds [14, 15]. For example, the stability of PdGa as a catalyst
17 in the semi-hydrogenation of acetylene to ethylene could be understood by analysing
18 the chemical bonding using the electron localizability indicator [16, 17]. In this
19 context it is worth mentioning, that the intermetallic compound PdZn (better to be
20 described as ZnPd, see the bonding analysis below) plays an important role as catalyst
21 in the steam reforming of methanol [18, 19]. The formation of the intermetallic
22 compound was detected *in situ* when applying Pd/ZnO as a catalyst, accompanied
23 with a huge increase in selectivity. The density of states of ZnPd and other
24 compounds realizing the CuAu or CsCl type of structures was used to draw
25 conclusions about their catalytic properties in the steam reforming of methanol [20].

26
27 In this study, the chemical bonding in the tetragonal and cubic structures of ZnPd is
28 explored using quantum chemical calculations through the electron localizability
29 indicator (ELI). Furthermore, new experimental data on the binary Pd-Zn phases
30 around 50 at.-% Pd are presented.

31 32 33 34 35 36 37 38 39 40 41 42 43 44 45 46 47 48 49 50 51 **Experimental**

52 53 54 *Synthesis of tetragonal ZnPd*

55
56 All procedures are carried out in an argon-filled glove box with H₂O and O₂
57 concentrations below 0.1 ppm. Elemental Zn (99.9999%, powder, ChemPur) and Pd
58 (99.9%, powder, Chempur) are weighed with a composition Zn₅₀Pd₅₀. The mixture is
59 filled in a quartz glass ampoule. After evacuating and sealing the tube, the ampoule is
60

1
2
3 placed in a furnace, and the temperature is increased with 5 K/h upon the melting
4 point of Zn (693 K) and finally raised to 1123 K with 1 K/min, where it is held for 6
5 days. The ampoule is cooled down and the sintered product is ground, sealed into an
6 evacuated quartz glass ampoule again and annealed at 1173 K for 7 days. After
7 quenching in water, the powder is analysed by X-ray powder diffraction (image plate
8 Guinier camera G670, Huber, Cu $K_{\alpha 1}$, $\lambda = 1.54056 \text{ \AA}$, quartz monochromator,
9 $3^\circ < 2\theta < 100^\circ$; internal standard LaB_6 , $a = 4.15692 \text{ \AA}$).

17 *Investigation of the homogeneity range of tetragonal ZnPd*

18
19 Samples containing 46 at.-% and 64 at.-% Pd, respectively, were prepared according
20 to the above synthesis route. The samples were finally annealed at 1173 K for 5 days.
21 After quenching in water, powders are analysed by X-ray powder diffraction and
22 WDX spectroscopy (CAMECA SX 100, W filament, 25 kV).

28 *Synthesis of cubic ZnPd*

30
31 To obtain the cubic (HT) modification of ZnPd, several quenching attempts were
32 made, all starting from a phase pure powder sample of tetragonal ZnPd. The challenge
33 is melting the compound while minimizing loss of zinc due to evaporation. The first
34 attempt consisted of heating the sample in a thin-walled closed quartz glass ampoule
35 to 1503 K, by referring to [11], followed by annealing for seven hours and finally
36 rapid quenching the ampoule in cold water. Another experiment to obtain the HT
37 modification started with inductive heating of the initial compound inside an open
38 glassy carbon crucible under inert argon atmosphere to 1673 K. After reaching this
39 temperature the crucible is turned upside down and the melt is poured onto a stainless
40 steel plate. Measuring the density of the quenched products by means of a Helium
41 pycnometer (AccuPyc 1330, Micromeritics) was used to obtain information about the
42 composition of the products.

54 *Quantum chemical calculations*

55
56 The tight-binding linear-muffin-tin-orbital (TB-LMTO) program [21] in the atomic
57 sphere approximation (ASA) and all-electron full-potential local orbital (FPLO)
58 scheme [22] are used for quantum chemical calculations on tetragonal and cubic
59 ZnPd. The issue of stability regarding the tetragonal and cubic crystal structures is
60

1
2
3 addressed by carrying out FPLO total energy calculations within local density (LDA)
4 and generalized gradient (GGA) approximations. For LDA *Perdew-Wang* [23] and for
5 GGA *Perdew-Burke-Ernzerhof* [24] parametrizations are used.
6
7

8
9 The following crystal structure model was used for tetragonal ZnPd: space group
10 *P4/mmm* (No. 123), Pd in Wyckoff position *1a* at 0 0 0, Zn in Wyckoff position *1d* at
11 0.5 0.5 0.5 with cell parameters $a = 2.8931(1) \text{ \AA}$ and $c = 3.3426(2) \text{ \AA}$ as determined
12 experimentally. Calculations on cubic ZnPd are based on the following structure
13 model: space group *Pm $\bar{3}$ m* (No. 221), Pd in *1a* at 0, 0, 0, Zn in *1b* at 0.5, 0.5, 0.5.
14 Since no experimental lattice parameter for cubic ZnPd is available at 50 at.-% Pd,
15 $a = 3.0513 \text{ \AA}$ was calculated by linear extrapolation of the cell parameters of cubic
16 Zn₃Pd₂ and cubic ZnPd₂ [10]. For LMTO-ASA calculations, no interstitial empty
17 spheres were necessary in either structure, because it was possible to reach the total
18 unit cell volumes by atomic spheres with acceptable overlap ($\leq 14\%$). The following
19 radii of the atomic spheres are applied for tetragonal ZnPd: $r(\text{Pd}) = 1.51 \text{ \AA}$,
20 $r(\text{Zn}) = 1.48 \text{ \AA}$. For cubic ZnPd, the applied radii of the atomic spheres are
21 $r(\text{Pd}) = 1.52 \text{ \AA}$, $r(\text{Zn}) = 1.49 \text{ \AA}$. The density of states (DOS) is calculated using a grid
22 of 55^3 k-points for tetragonal ZnPd and 58^3 k-points for cubic ZnPd, respectively.
23
24 Chemical bonding analysis is based on the concept of electron localizability. The
25 electron localizability indicator (ELI, λ) [25] is evaluated in ELI-D according to [26,
26 27]. ELI can be calculated by both FPLO [28] and TB-LMTO methods. The topology
27 of ELI is analysed using the program DGrid [29] with integration of the electron
28 density in ELI basins, a procedure similar to that in the quantum theory of atoms in
29 molecules (QTAIM) proposed by Bader [30].
30
31
32
33
34
35
36
37
38
39
40
41
42
43
44
45

46 **Results and discussion**

47 *Synthesis of tetragonal and cubic ZnPd*

48
49
50
51 Single phase material of tetragonal ZnPd was obtained after annealing the pre-reacted
52 powder at 1173 K as confirmed by X-ray powder diffraction (Fig. 1). The compound
53 is hard and brittle with silvery metallic lustre. Contrary to previously reported
54 synthesis routes which always had to deal with evaporating zinc, this method is
55 capable of preparing the compound with the initial equiatomic Pd:Zn ratio. The cell
56 parameters were determined as $a = 2.8931(1) \text{ \AA}$ and $c = 3.3426(2) \text{ \AA}$. The samples for
57 the homogeneity range determination consisted of tetragonal ZnPd and cubic ZnPd₂
58
59
60

1
2
3 or cubic Zn_3Pd_2 , respectively, in accordance to the published phase diagram. Unit cell
4 parameters as well as the composition of ZnPd in the mixtures are shown in Table 1.
5
6 The synthesis of cubic ZnPd in an open glassy carbon crucible, quenched from melt,
7 only yielded zinc poor samples with compositions of $Zn_{0.66}Pd_{1.34}$ (according to the
8 density measurements) due to evaporation of zinc. The evaporation of zinc can be
9 avoided if the initial compound is placed inside a quartz glass ampoule which then is
10 quenched from 1503 K. Nevertheless, single phase material of tetragonal ZnPd was
11 obtained instead of cubic ZnPd. Hence, the existence of cubic ZnPd (50 at.-% Pd)
12 could not be proven experimentally using the preparation procedures applied.
13
14
15
16
17
18
19
20

21 *On the stability of the cubic structure*

22
23 Since $c/a = 1$ in the tetragonal space group $P4/mmm$ gives the cubic structure, total
24 energy calculations in that space group were performed to compare the energies for
25 different c/a ratios at a given unit cell volume. The results obtained by GGA at the
26 experimental volume of the unit cell are shown in Fig. 2. The lowest total energy is
27 obtained at the experimental c/a value of ~ 1.155 , while the energy of the cubic
28 structure ($c/a = 1$) is higher by ~ 10 meV/atom. To determine the volume dependence
29 of the c/a ratio, the c/a ratios of the tetragonal structure are optimized for different
30 unit cell volumes by both LDA and GGA (Fig. 2). In both cases, c/a decreases
31 monotonically with decreasing volume, but even at a volume compression of $\sim 35\%$,
32 the c/a ratio is around 1.09, far from the cubic limit of 1. These results suggest that at
33 larger volumes, which should be attained at elevated temperatures due to thermal
34 expansion, the lowest total energies will be obtained at larger c/a values, which is in
35 clear contradiction to the assumption that the tetragonal structure will transform to the
36 cubic structure at higher temperatures. The theoretical equilibrium volume obtained
37 by GGA (LDA) is 3.8% larger (4.5% smaller) than the experimental volume. Both
38 results are within the expected range of deviations for each functional.
39
40
41
42
43
44
45
46
47
48
49
50

51 As would be expected for both compounds, the major contributions in the DOS
52 originate from the Zn- d and Pd- d states (TB-LMTO-ASA results, Fig. 3). The main
53 difference in the density of states is detected around the Fermi energy. In the cubic
54 structure a higher contribution by Pd- d states to the DOS at the Fermi energy is
55 observed, compared to the tetragonal structure. The local peak in the density of states
56 close below the Fermi energy indicates a possible instability of the cubic crystal
57
58
59
60

1
2
3 structure in agreement with the total energy calculations. In tetragonal ZnPd, this local
4 peak close to the Fermi energy splits into two smaller peaks at -1 eV and +0.5 eV,
5 respectively. This change in the electronic structure suggests a Peierls-like distortion
6 stabilising the tetragonal structure in ZnPd.
7

8
9
10 The topology of calculated electron density for both, the cubic and the tetragonal
11 structure, reveals very similar basins defined by the zero-flux surfaces in the density
12 gradient, the QTAIM atoms (Fig. 4, top). The volume of the QTAIM Pd (16.65 \AA^3) is
13 smaller than the average value of 22.3 \AA^3 between the atomic volumina of the
14 elemental palladium (29.4 \AA^3) and zinc (15.2 \AA^3). The volume of QTAIM Zn (11.32
15 \AA^3) is even smaller than for metallic zinc. In the chemically similar system Al-Pt [31]
16 this indicated atomic interactions between the components and formation of Pt anions
17 and Al cations. Indeed, integration of the electron density within the QTAIM reveals
18 charge transfer from Zn to Pd for both structures and both calculation methods, in
19 accordance with their electronegativities after Pauling [32]. Following the IUPAC
20 nomenclature, we therefore suggest to describe the compound as ZnPd. Integration of
21 the electron density obtained by the FPLO calculation yields $\text{Zn}^{0.4+}\text{Pd}^{0.4-}$, revealing the
22 important role of the charge transfer in the formation of the cubic and tetragonally
23 distorted body-centred-like structural patterns in the system Zn-Pd.
24

25
26 The reasons for the tetragonal distortion are visualized by the analysis of the electron
27 localizability indicator for both structural motifs (Fig. 4, middle and bottom). For both
28 structures, the distribution of ELI-D in the inner shells (especially the penultimate
29 third one) around the zinc nuclei is very close to spherical. The basins of the ELI
30 attractors in the valence region are multi-synaptic implying multi-centre Zn-Pd
31 bonding interactions (not shown in the figure). In combination with the charge
32 transfer, this suggests polar interaction between Zn and Pd. Contrary to zinc, in the
33 tetragonal structure the penultimate shell of palladium is significantly structured in the
34 (001) plane compared to weaker structuring in the (100) plane. Such a structuring
35 proved to be a fingerprint for the direct (covalent) interaction between the palladium
36 atoms [33, 34]. This interaction is also reflected by small ELI-D maxima between the
37 Pd atoms along [100] (Fig. 4, middle). In cubic ZnPd, the structuring is less
38 pronounced as illustrated by the structuring index (the difference between the highest
39 ELI-D value in the examined shell and the ELI-D value at which the localization
40 domain is without a "hole" [35] which is 0.037 for the tetragonal structure and 0.012
41 for the cubic one). Furthermore, no maxima in ELI-D were calculated between the Pd
42
43
44
45
46
47
48
49
50
51
52
53
54
55
56
57
58
59
60

1
2
3 atoms. Thus, the direct Pd-Pd bonding within the 4⁴ nets in the (001) plane is the main
4
5 reason for the tetragonal distortion of the cubic structure in case of ZnPd.
6
7

8 **Conclusions**

9
10 The existence of the cubic high-temperature phase of equiatomic composition in the
11
12 binary system Pd-Zn could not be proven experimentally and remains uncertain.

13 Tetragonal ZnPd possesses a homogeneity range of 13.8 at.-% at 1173 K.

14
15 Calculations of the total energy reveal a minimum at $c/a = 1.155$, clearly excluding
16
17 the cubic pattern at the equiatomic composition in the system Zn-Pd. Analysis of the
18
19 chemical bonding applying the electron localizability approach revealed the charge
20
21 transfer from Zn to Pd, justifying the formula ZnPd instead of PdZn. In addition,
22
23 direct Pd-Pd interactions in the (001) plane were shown to be the main reason for the
24
25 tetragonal distortion of cubic ZnPd.
26
27
28
29
30
31
32
33
34
35
36
37
38
39
40
41
42
43
44
45
46
47
48
49
50
51
52
53
54
55
56
57
58
59
60

References

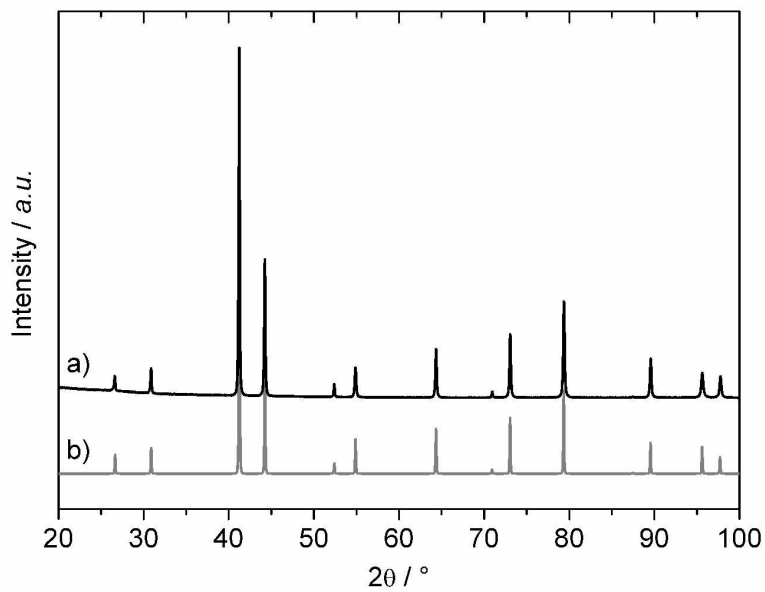
- [1] C.H. Johansson, J.O. Linde, *Ann. Phys.* 78, **1925**, 439.
- [2] K. Schubert, *Z. Metallkde.* 46, **1955**, 43.
- [3] T. Muto, *Sci. Pap. Inst. Phys. Chem. Res. Tokyo* 34, **1938**, 377.
- [4] U. Dehlinger, *Z. Phys.* 105, **1937**, 588.
- [5] J.P. Neumann, H. Ipsier, Y.A. Chang, *J. Less-Comm. Met.* 57, **1978**, P29.
- [6] Z.W. Lu, A. Zunger, A.G. Fox, *Acta Metall. Mater.* 42, **1994**, 3929.
- [7] J. Braun, M. Ellner, B. Predel, *Z. Metallkde.* 86, **1995**, 870.
- [8] W.K. Wang, H. Iwasaki, *J. Phys. Chem. Solids* 48, **1987**, 559.
- [9] H. Nowotny, H. Bittner, *Monatshefte für Chemie* 81, **1950**, 679.
- [10] H. Nowotny, E. Bauer, A. Stempf, *Monatshefte für Chemie* 82, **1951**, 1086.
- [11] W. Köster, U. Zwicker, *Festschrift 100 Jahre W.C. Heräus, Hanau*, **1951**, 76.
- [12] T.B. Massalski, *Binary Alloy Phase Diagrams*, 2nd Edition, ASM International, **1990**.
- [13] M. Hansen, K. Anderko, *Constitution of Binary Alloys*, 2nd Edition, McGraw-Hill Book Company, **1958**.
- [14] M. Armbrüster, W. Schnelle, U. Schwarz, Yu. Grin, *Inorg. Chem.* 46, **2007**, 6319.
- [15] K. Kovnir, M. Armbrüster, D. Teschner, T.V. Venkov, F.C. Jentoft, A. Knop-Gericke, Yu. Grin, R. Schlögl, *Sci. Technol. Adv. Mater.* 8, **2007**, 420.
- [16] J. Osswald, R. Giedigkeit, R.E. Jentoft, M. Armbrüster, F. Girgsdies, K. Kovnir, T. Ressler, Yu. Grin, R. Schlögl, *J. Catal.* 258, **2008**, 210.
- [17] J. Osswald, K. Kovnir, M. Armbrüster, R. Giedigkeit, R.E. Jentoft, U. Wild, Yu. Grin, R. Schlögl, *J. Catal.* 258, **2008**, 219.
- [18] N. Takezawa, N. Iwasa, *Cat. Today* 36, **1997**, 45.
- [19] K.M. Neyman, K.H. Lim Z.-X. Chen, L.V. Moskaleva, A. Bayer, A. Reindl, D. Borgmann, R. Denecke, H.-P. Steinrück, N. Rösch, *Phys. Chem. Chem. Phys.* 9, **2007**, 3470.
- [20] A.P. Tsai, S. Kameoka, Y. Ishii, *J. Phys. Soc Japan* 73, **2004**, 3270.
- [21] O. Jepsen, A. Burkhardt, O.K. Andersen, *The Program TB-LMTO-ASA*, Version 4.7, Max-Planck-Institut für Festkörperforschung, Stuttgart, **1999**.
- [22] K. Koepernik, H. Eschrig, *Phys. Rev. B* 59, **1999**, 1743; for more information: www.fplo.de.

- 1
2
3
4 [23] J.P. Perdew, Y. Wang, *Phys. Rev. B* 45, **1992**, 13244.
5
6 [24] J.P. Perdew, K. Burke, M. Ernzerhof, *Phys. Rev. Lett.* 77, **1996**, 3865.
7
8 [25] M. Kohout, *Int. J. Quantum. Chem.* 97, **2004**, 651.
9
10 [26] M. Kohout, F.R. Wagner, Yu. Grin, *Int. J. Quantum Chem.* 106, **2006**, 1499.
11
12 [27] M. Kohout, *Faraday Discuss.* 135, **2007**, 43.
13
14 [28] A. Ormeci, H. Rosner, F.R. Wagner, M. Kohout, Yu. Grin, *J. Phys. Chem. A*
15 *110*, **2006**, 1100.
16
17 [29] M. Kohout, *DGrid*, Version 4.5, Max-Planck-Institut für Chemische Physik
18 fester Stoffe , Dresden, **2010**.
19
20 [30] R.F.W. Bader, *Atoms in Molecules: A Quantum Theory*, Oxford University
21 Press, Oxford, **2003**.
22
23 [31] A. Baranov, M. Kohout, F.R. Wagner, Yu. Grin, W. Bronger, *Z. Kristallogr.*
24 *222*, **2007**, 527.
25
26 [32] J. Emsley, *The Elements*, Clarendon Press, Oxford, **1991**.
27
28 [33] M. Kohout, F.R. Wagner, Yu. Grin, *Theor. Chem. Acc.* 108, **2002**, 150.
29
30 [34] F.R. Wagner, V. Bezugly, M. Kohout, Yu. Grin, *Chem. Eur. J.* 13, **2007**, 5724.
31
32
33
34
35
36
37
38
39
40
41
42
43
44
45
46
47
48
49
50
51
52
53
54
55
56
57
58
59
60

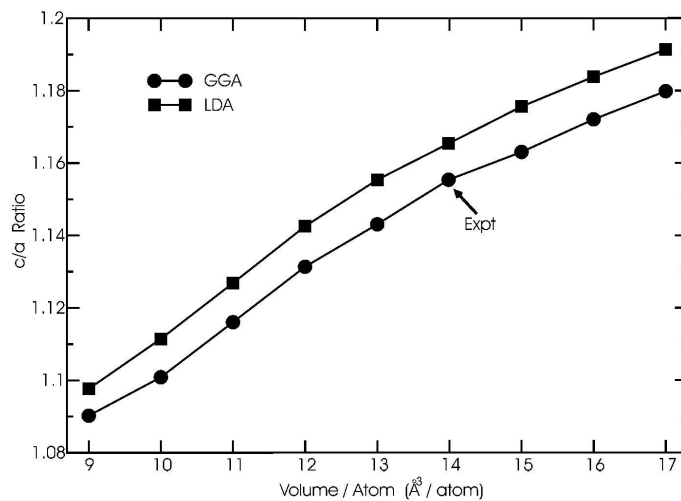
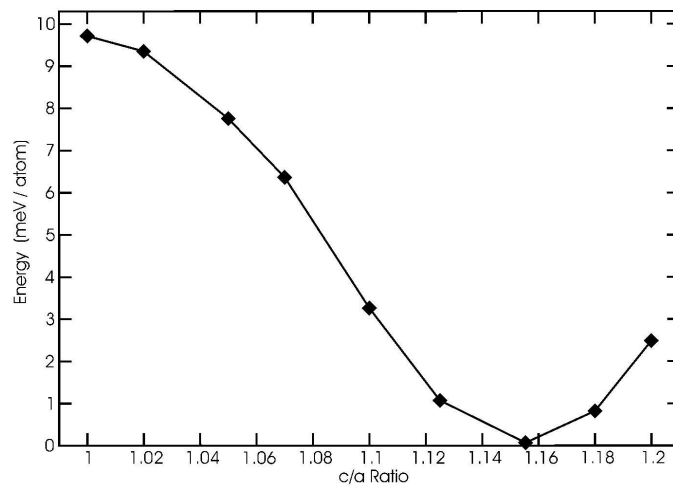
Tables

Table 1: Composition and lattice parameters of the tetragonal ZnPd phase in the two-phase samples

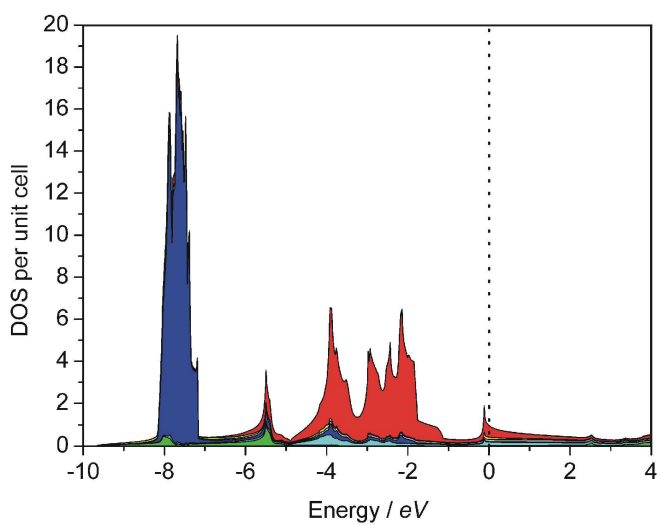
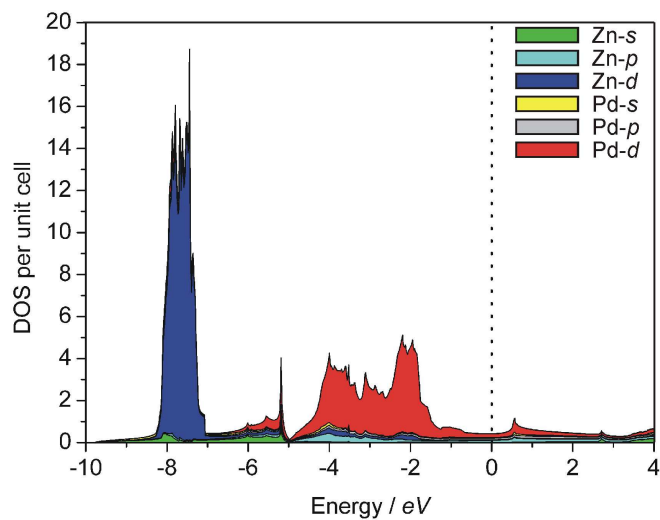
Initial composition / at.-%	Composition by WDXS / at.-%	Lattice parameters / Å		
Zn ₃₆ Pd ₆₄	Zn _{37.1} Pd _{62.9}	$a = 2.9532(6)$	$c = 3.269(1)$	$c/a = 1.107$
Zn ₅₄ Pd ₄₆	Zn _{50.9} Pd _{49.1}	$a = 2.8878(2)$	$c = 3.3622(3)$	$c/a = 1.164$



(a) Experimental and (b) calculated X-ray powder diffraction pattern of tetragonal ZnPd.
573x398mm (150 x 150 DPI)

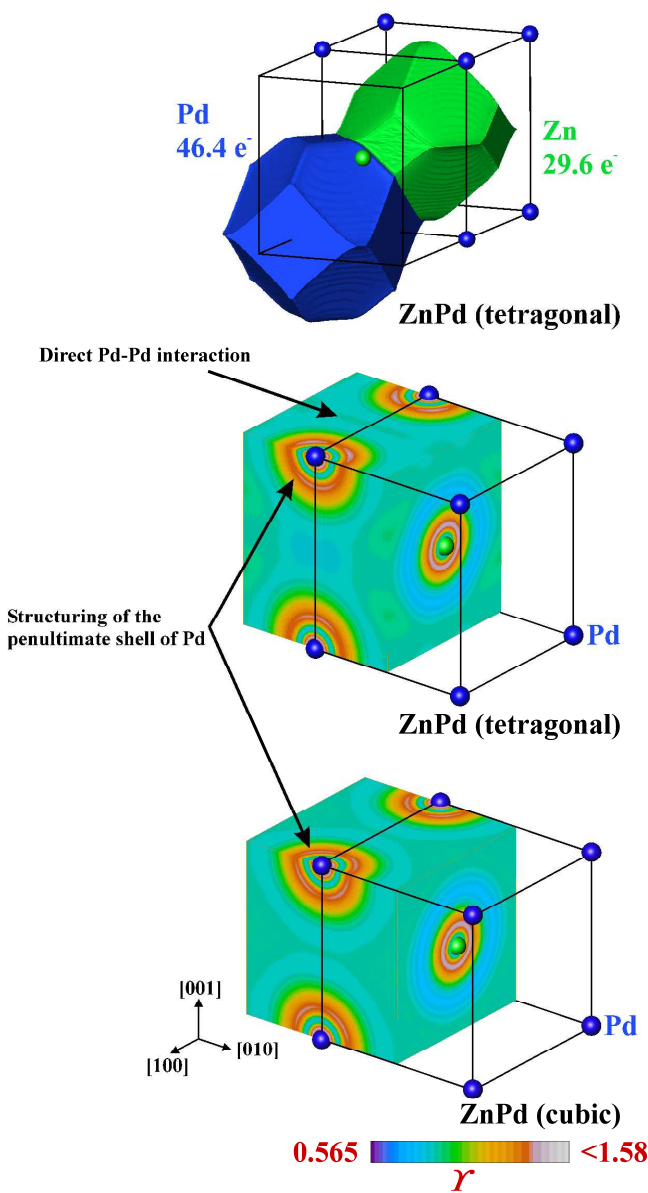


(top) Total energy per atom vs. c/a ratio is obtained within GGA for tetragonal ZnPd at the experimentally observed unit cell volume of 13.989 \AA^3 . The minimum was observed at the experimental c/a value of ~ 1.155 , the cubic structure with $c/a = 1$ has a much higher energy. (bottom) Axial ratio c/a vs. unit cell volume for GGA and LDA calculations (bottom). The arrow marks the experimentally determined c/a ratio and volume.



48 Total and partial electronic DOS for tetragonal ZnPd (CuAu-type, top) and cubic ZnPd (CsCl-type,
49 as obtained by TB-LMTO-ASA.

50
51
52
53
54
55
56
57
58
59
60



Chemical bonding in ZnPd: (top) QAIM basins of Pd (blue) and Zn (green) in tetragonal ZnPd (FPLO calculation) with the according electronic populations revealing the charge transfer from Zn to Pd. (middle) ELI-D distribution in the (100), (010) and (001) planes in tetragonal ZnPd shows strong structuring of the penultimate shell of Pd in the (001) plane as well as small ELI-D maxima between Pd atoms along [100]. (bottom) ELI-D distribution in the (100), (010) and (001) planes in cubic ZnPd shows weaker structuring of the penultimate shell of Pd in all three planes.
155x292mm (600 x 600 DPI)